Spin Polarization of Conduction Electrons in Gd†

R. M. Moon and W. C. Koehler
Solid State Division, Oak Ridge National Laboratory, Oak Ridge, Tennessee 37830
(Received 2 June 1971)

Neutron diffraction measurements on single crystals of ^{160}Gd have been performed which allow the reconstruction, by Fourier synthesis, of the magnetization as a function of position. It is shown that the total magnetic moment density can be separated in a logical manner into a local part and a diffuse part. It is suggested that the local part corresponds to the $4f$ polarization and the diffuse part to the conduction-electron polarization. Contour maps show the diffuse contribution to be long range and oscillatory.

The existence of a large spin polarization in the conduction band of metallic Gd is well established. The $4f$ shell is half full for Gd so we expect a magnetic moment of $7\mu_B$ per atom, but magnetization measurements by Nigh, Legvold, and Spedding[1] on the ferromagnetic metal gave an atomic moment of $7.55\mu_B$. This excess moment of $0.55\mu_B$ is generally attributed to spin polarization in the conduction band. The purpose of this Letter is to present evidence on the spatial distribution of this excess moment based on neutron diffraction measurements.

This is one aspect of a rather complete investigation of the spatial distribution of magnetic moment in Gd. Because there is no orbital moment in the case of Gd, the magnetic-moment density is proportional to the unpaired spin density. A full report is in preparation and preliminary reports of other aspects of the work have been published.[2,3] Measurements of the magnetic scattering amplitude of ferromagnetic ^{160}Gd have been performed at 96°K using both polarized and unpolarized neutrons. Data have been obtained for all $(hk0)$ Bragg peaks out to $\sin\theta/\lambda = 1.275$ and for all $(0kl)$ peaks out to $\sin\theta/\lambda = 1.04$. A portion of these data are presented in Fig. 1. We believe the abrupt change in slope at $\sin\theta/\lambda = 0.18$ is associated with the conduction-electron polarization. The problem we wish to discuss is how to separate the $4f$ contribution to the data of Fig. 1 from that of the conduction electrons.

If there were reliable calculations of the $4f$ form factor, it would be possible to obtain the conduction contribution by subtraction. However, examination of the complete set of data shows that the metallic $4f$ form factor is significantly different from the free-ion calculation of Blume, Freeman, and Watson.[4] Rather than relying on a specific calculation to effect the desired separation, we have attempted to make this separation based on very simple and general ideas about how these two contributions should behave. Specifically, we assume that in real space the $4f$ contribution is highly localized and that the conduction contribution is spread throughout the unit cell. To be properly cautious, we will call these two contributions local and diffuse since it is these properties which we will use in making the separation.

Basic to our interpretation is the assumption that the total periodic magnetic moment density, $\rho_T(\vec{r})$, can be separated into a local part, $\rho_L(\vec{r})$, and a diffuse part, $\rho_D(\vec{r})$:

$$\rho_T(\vec{r}) = \rho_L(\vec{r}) + \rho_D(\vec{r}). \quad (1)$$

All three of these functions have the periodicity of the lattice and so each may be written as a Fourier series:

$$\rho_\alpha(\vec{r}) = V^{-1}\sum_j F_{\alpha j} \exp(-i\vec{k}_j\cdot\vec{r}), \quad (2)$$

where V is the unit cell volume, α runs over the set of subscripts in Eq. (1), and j runs over all reciprocal lattice points. Our measurements give the set of coefficients F_{Tj}. If $\rho_D(\vec{r})$ is a slowly varying function of $\vec{r}$, only the first few terms in the Fourier series describing this func-

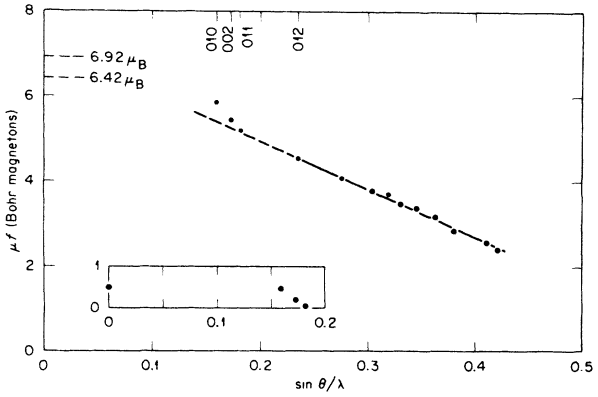

FIG. 1. Magnetic scattering amplitudes for low-angle reflections in Gd. Experimental errors are indicated by the size of the data-point circles. Insert shows scattering amplitudes for the diffuse contribution.

tion will be nonzero. Inspection of Fig. 1 suggests that only the first three reflections, in addition to the total moment, are affected by $\rho_D(\vec{r})$. We assume that $F_{Dj}=0$ for $\sin\theta/\lambda \geq 0.235$, and therefore $F_{Lj}=F_{Tj}$ in this range of $\sin\theta/\lambda$. The only requirement we impose on $\rho_L(\vec{r})$ is that it be sufficiently localized so that overlap between neighboring sites is negligible. More simply, we require that $\rho_L(\vec{r})\approx 0$ for a reasonably large range of values of $\vec{r}$ away from atomic sites. The procedure to follow is now clear. We will try to adjust the scattering amplitudes for the first three Bragg reflections so that when they are combined with the rest of the data in a Fourier series, a constant value of $\rho_L(\vec{r})$ is obtained in the region between atoms. If this can be done, the integral under this local distribution can be determined by the method described by Moon,[5] or equivalently, $F_L(000)$ can be adjusted so that $\rho_L(\vec{r})=0$ for $\vec{r}$ away from the atomic sites. To be convincing, this procedure should yield a value for the local moment in agreement with our expectation based on the magnetization measurement. At the experimental temperature of 96°K and applied field of 12.5 kOe the total magnetic moment is $6.92\mu_B$.[1] If we assume that the $4f$ contribution has the same temperature dependence as the total moment, we expect a $4f$ moment of $6.42\mu_B$.

We do not have complete three-dimensional data so that we cannot calculate the local point density. However, using the set of reflections $(hk0)$ we can calculate the projected density onto the basal plane and using the $(0kl)$ reflections we can calculate the projected density onto the plane perpendicular to the hexagonal a axis. For these calculations we have represented the hexagonal close-packed structure in terms of an orthorhombic cell with lattice constants $a=3.626$, $b=6.280$, and $c=5.797$. The atomic positions are $(0, \frac{1}{3}, \frac{3}{4})$, $(0, \frac{2}{3}, \frac{1}{4})$, $(\frac{1}{2}, \frac{1}{6}, \frac{1}{4})$, and $(\frac{1}{2}, \frac{5}{6}, \frac{3}{4})$. The basal plane projection is particularly favorable for examining the behavior of $\rho_L(\vec{r})$ in the region between atoms. For this projection we have only the $(010)_{hex}$ amplitude as an adjustable parameter. To avoid series termination errors we calculate the average density over a suitable volume centered at the point $\vec{r}$ and then project this averaged density onto the basal plane. The geometry of the situation (see Fig. 2) suggests that a spherical average be used. The appropriate formulas for this averaging have been previously given.[5]

In Fig. 2 we show the results of such a calculation for three different values of the $(010)_{hex}$ amplitude. The top curve shows $\rho_T(\vec{r})$ using the observed $(010)_{hex}$ amplitude shown in Fig. 1. It is clear that this total moment density does not have the desired local character. The negative values at large distance show that the diffuse component must be oscillatory, since the magnetization measurement gives a positive average value. For the second curve the $(010)_{hex}$ amplitude has been decreases to fall on the extrapolated linear portion of Fig. 1. The calculation now shows beautiful local behavior. Furthermore, the local moment calculation[5] giving the integral of the moment density above the flat region yields a local atomic moment of $(6.44 \pm 0.16)\mu_B$, in excellent agreement with the expected value of $6.42\mu_B$. This agreement is also obvious from the dashed line indicating the zero on the density scale for an average moment of $6.42\mu_B$. The bottom curve is included merely

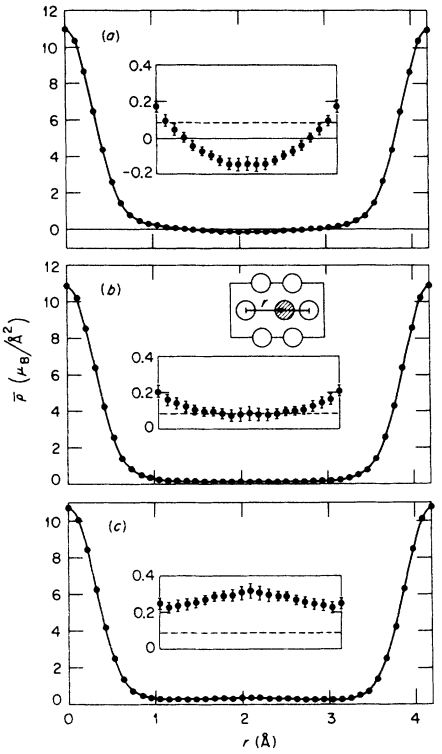

FIG. 2. Projection of spherically averaged moment density onto basal plane as a function of distance from atomic site. The averaging sphere, of radius 0.63 Å, is moved along the line indicated in the structural diagram. In (a), $(\mu f)_{010}=5.854$; in (b), $(\mu f)_{010}=5.400$; and in (c), $(\mu f)_{010}=4.945$. Inserts show density near the center of the cell on an expanded scale. Dashed lines show the zero density level if the average moment per atom is $6.42\mu_B$. Error bars show the standard deviation obtained by combining the statistical errors in individual scattering amplitudes.

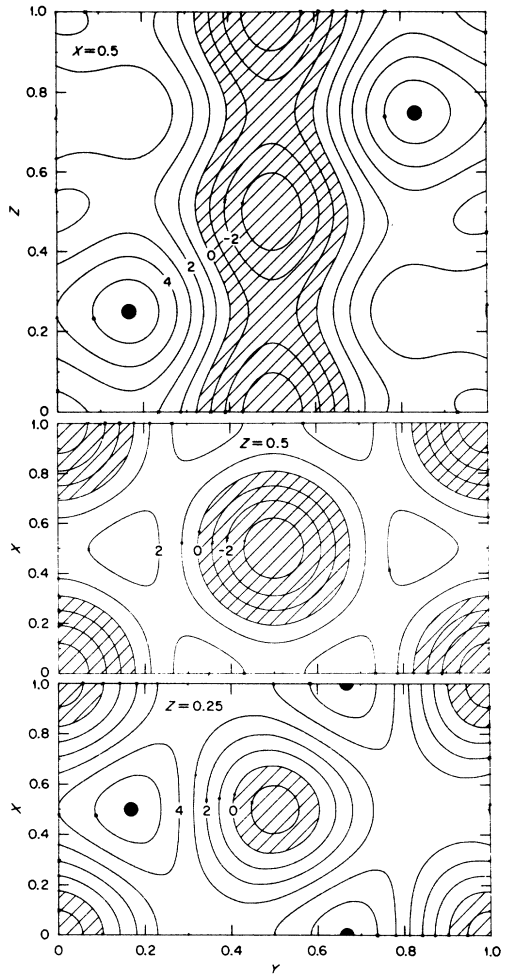

FIG. 3. Contour maps of diffuse component of magnetic moment density. Shaded areas have negative density values. Numbers on contour lines are multiples of $0.01\mu_B/\text{Å}^3$ or multiples of 1.16 kG. Atomic sites are indicated by black circles. Errors vary from $\frac{1}{2}$ contour interval to about a full interval.

to give an idea of the sensitivity of the method. We have here overcorrected the $(010)_{hex}$ amplitude by moving it below the linear extrapolation in Fig. 1 and the result clearly does not satisfy our criterion for local behavior. Similar calculations using the $(0kl)$ set of reflections show that the amplitudes of the second and third reflections should be decreased to fall on the linear extrapolation in Fig. 1 in order to describe a local density function.

The contribution of the diffuse component to the scattering amplitudes is given by the difference between the experimental results and those describing the local component. This difference is shown in the insert of Fig. 1. By definition, this is a complete set of Fourier amplitudes and we can proceed to calculate the point density of the diffuse component throughout the unit cell. Contour maps giving the diffuse magnetization in several interesting planes are shown in Fig. 3. At each atomic site there is a maximum density of magnitude $(0.056 \pm 0.012)\mu_B/\text{Å}^3$ (6.6 kG) parallel to the local moment. As you move away from the atomic sites the polarization direction reverses, reaching a maximum of $(-0.037 \pm 0.004)\mu_B/\text{Å}^3$ (−4.4 kG). Undulating columns of negative polarization run continuously through the lattice parallel to the c axis. If the crystal structure is described in terms of stacking of close-packed layers, the atomic sites are in an $ABAB\cdots$ sequence and the columns of negative polarization run through the C sites.

There seems little doubt that we have successfully split the total magnetization into a local part and a diffuse part. The further step of identifying the local contribution with the $4f$ electrons and the diffuse contribution with the conduction electrons should be taken cautiously. The most compelling evidence in favor of this interpretation is the excellent agreement we get with the expected $4f$ moment by integrating under our local moment distribution. As already indicated, our data are not in good agreement with nonrelativistic Hartree-Fock calculations[4] for the $4f$ electrons in Gd^{3+}. This statement is true independent of the details of the separation between the local and diffuse parts. However, there is an argument that can be made to show that the separation we have used is consistent with certain general properties of calculated ionic $4f$ form factors. For small values of $\sin\theta/\lambda$, atomic form factors have the functional form

$$f = 1 - A(\sin\theta/\lambda)^2. \quad (3)$$

For higher values of $\sin\theta/\lambda$ the curvature is positive and there is an intermediate region where the curvature is close to zero. This nearly linear region occurs roughly from 0.2 to 0.4 in $\sin\theta/\lambda$ for the rare-earth $4f$ electrons.[4] So we have a form factor which, to a very good approximation, has an initial region of quadratic behavior followed by a region of linear behavior. Knowing the slope in the linear region and the zero intercept in the quadratic region, and requiring the functions and first derivatives to be equal at the boundary between the two regions, it is easy to calculate the value of $\sin\theta/\lambda$ corresponding to this boundary. We have performed this calcula-

tion for all the $\langle j_0 \rangle$ functions given by Blume, Freeman, and Watson.[4] In each case we can accurately predict where the departure from linearity begins to be comparable to our experimental error. Applying the same analysis to the experimental data on Gd, we find that the linear region of Fig. 1 should extend to $\sin\theta/\lambda = 0.143$, which is inside the first Bragg reflection. We conclude that our local form factor has behavior consistent with that of calculated $4f$ form factors in the questionable region.

Theoretical calculations are not sufficiently advanced to judge whether our diffuse component behaves exactly as conduction electrons should. The form factor shown in the Fig. 1 insert is not similar to that expected for $6s$ or $5d$ electrons in atomic Gd, nor does it correspond to the spin polarization produced in free electrons by the Ruderman-Kittel-Kasuya-Yosida interaction. Note that for three free electrons in Gd, the $\sin\theta/\lambda$ value corresponding to twice the Fermi wave vector ($2k_F$) is 0.222 Å^{-1}. However, our diffuse component is certainly long range and oscillatory, which are properties universally attributed to conduction electrons in the rare-earth metals.

*Research sponsored by the U. S. Atomic Energy Commission under contract with Union Carbide Corporation.

[1]H. E. Nigh, S. Legvold, and F. H. Spedding, Phys. Rev. 132, 1092 (1963).
[2]W. C. Koehler, R. M. Moon, J. W. Cable, and H. R. Child, J. Phys. (Paris), Suppl. 32, C1-296 (1971).
[3]R. M. Moon, W. C. Koehler, J. W. Cable, and H. R. Child, J. Appl. Phys. 42, 1303 (1971).
[4]M. Blume, A. J. Freeman, and R. E. Watson, J. Chem. Phys. 37, 1245 (1962).
[5]R. M. Moon, Int. J. Magn. 1, 219 (1971).

Intense Tunable Phonon Fluorescence in Superconductors

V. Narayanamurti and R. C. Dynes
Bell Telephone Laboratories, Murray Hill, New Jersey 07974
(Received 21 June 1971

The "phonon fluorescence" spectrum of superconducting Sn and $Pb_{0.5}Tl_{0.5}$ films pumped by a heat pulse is studied through the observation of resonance absorption by Sb donor levels in uniaxially compressed Ge. The spectrum consists primarily of a narrow band of phonons centered about the energy gap 2Δ (1.2 meV for Sn, 1.7 meV for $Pb_{0.5}Tl_{0.5}$). The power generated in this narrow band is at least hundreds of milliwatts. In the case of Sn the phonon energy has been tuned from 1.2 meV down to 0.7 meV by a magnetic field parallel to the plane of the film.

It was first pointed out by Eisenmenger and Dayem[1] that superconducting tunnel junctions could be used for the quantum generation of incoherent phonons with frequencies up to about 10^{12} Hz. In a recent Letter[2] (hereafter referred to as I) we measured the frequency spectrum of phonons emitted by a tunnel junction into a solid and showed that such junctions could be used to generate a much higher power level of effectively monochromatic phonons (of energy 2Δ, the superconducting energy gap) than previously envisioned. This realization made the device of potential use for the study of high-frequency monochromatic phonon transport and interactions in materials. In this Letter we report a new, more intense, simpler method for the generation of these phonons and describe the successful attempt to tune the emitted phonon frequency over a wide range. This tuning of both generator and detector is achieved by the application of a parallel magnetic field ($\lesssim 1$ kG), which adjusts the superconducting energy gap 2Δ controlling the frequency of emitted phonons.

From I it was clear that to generate phonons whose spectrum shows a peak at 2Δ it was not necessary to employ a tunnel junction. It was shown that phonons (generated by the relaxation of high-energy injected quasiparticles) whose energies $\hbar\omega > 2\Delta$ are extremely short lived. They rapidly break Cooper pairs, thus creating quasiparticle excitations above the energy gap. These quasiparticles then relax to the gap edge by emitting phonons and the process repeats until the generated phonons have energies $< 2\Delta$ at which time they become discontinuously long lived. The excitations at the gap edge subsequently recom-